Second International Conference on CFD in the Minerals and Process Industries
CSIRO, Melbourne, Australia
6-8 December 1999

ANALYSIS OF PERFORMANCE OF AN IRON-BATH REACTOR USING COMPUTATIONAL FLUID DYNAMICS

Vladimir PANJKOVIC[1], John TRUELOVE[2] and Oleg OSTROVSKI[3]

[1] formerly: Steel Research Laboratories, BHP Steel, PO Box 202, Port Kembla NSW 2505, AUSTRALIA
now: BHP Information Technology, Level 32, 600 Bourke St., Melbourne VIC 3000, AUSTRALIA
[2] Centre for Metallurgy and Resource Processing, BHP Minerals, PO BOX 188, Wallsend NSW 2287, AUSTRALIA
[3] School of Materials Science and Engineering, The University of NSW, Sydney NSW 2052, AUSTRALIA

ABSTRACT

The performance of an iron-bath reactor has been studied using a comprehensive numerical model which combines a computational fluid dynamics approach for the gas phase and a heat and mass balance model for the bath. The model calculates:

- Coal, ore, flux and oxygen consumption;
- Post-combustion ratio;
- Heat-transfer efficiency;
- Off-gas temperature and composition;
- Heat transfer and chemical reactions between gas and iron and slag droplets; and
- Heat transfer between gas and bath, refractories and lance.

The model was validated with data reported for a 100 t pilot plant. On the basis of modelling results, the dominant mechanisms of heat transfer from the gas to the bath are radiation to the slag surface and convection heat transfer to droplets.

NOMENCLATURE

C_p	heat capacity
D	diffusion coefficient
G	shear production
H	enthalpy
k	turbulent kinetic energy
p	pressure
S_d	source term due to gas-dust heat transfer
S_D	source term due to gas-droplets heat transfer
S_m	mass source due to gas-droplets chemical reactions
S_{rad}	source term due to radiation
S_u	source term due to particle momentum
S_y	source term due to chemical reactions in gas phase
u_G	gas velocity
y_i	mass fraction of the *i*-th species in the gas phase
ε	rate of dissipation of turbulent energy
ζ	bulk viscosity
λ_G	thermal conductivity of gas
μ_{eff}	effective viscosity
μ_L	laminar viscosity
μ_T	turbulent viscosity
ρ_G	gas density

INTRODUCTION

Production of iron has been dominated for decades by the traditional route consisting of coke ovens, ore agglomeration plant and blast furnace. Despite its dominance, the route has two drawbacks: it requires large-scale production to be profitable and preparation of raw materials. The iron-bath reactor is an alternative process which can eliminate these issues. In this process (Fig. 1), coal, oxygen, ore and fluxes are charged to the bath. Oxygen or preheated air is blown into the freeboard for post combustion of carbon monoxide and hydrogen released from the bath. Slag and iron droplets are ejected from the bath into the gas phase, where they are heated before returning to the bath. Iron droplets undergo decarburisation and reoxidation by carbon dioxide and steam, while iron oxide in slag droplets is oxidised to Fe_2O_3. Dust is blown from the bath, and the bath may be stirred with bottom injected gas.

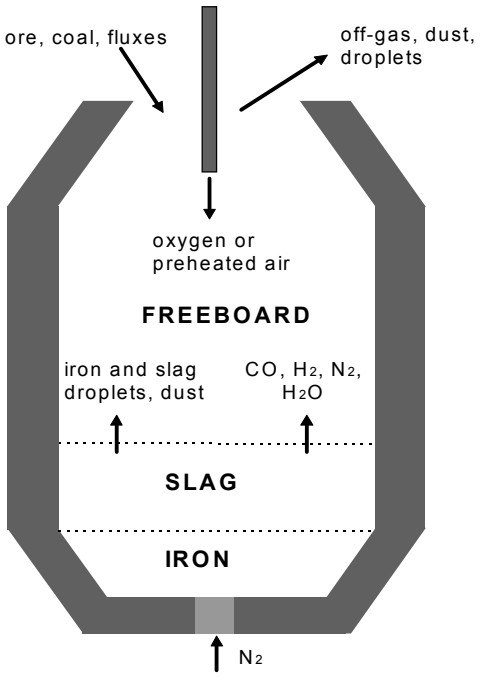

Figure 1: A schematic of a typical iron-bath reactor.

In iron-bath reactors, fuel efficiency is improved by post combustion and efficient transfer of the generated heat to the bath. As large-scale experimental equipment is expensive, mathematical models provide a cost-effective means for investigation of these factors. Relatively simple models, which did not consider the spatial variations in the gas phase, gave useful information about the process performance (Fruehan et al., 1989; Xu and Holappa, 1990; Ai et al., 1990; Zhang and Oeters, 1991, 1993; Sampaio et al., 1992; Panjkovic et al., 1996). However, development of CFD models is warranted since significant spatial variations of gas properties in the freeboard of these reactors exist. Several relevant CFD models have been reported in the literature (Gou et al., 1993; Shinotake and Takamoto, 1993; Shin et al., 1993; Schwarz and Davis, 1993; Tanski, 1994; Li et al., 1996; Becker-Lemgau and Tacke, 1996; Zhang and Oeters, 1996; Davis et al., 1997). However, only Shinotake and Takamoto (1993) took into account the effect of raw material properties. Heat transfer from gas to droplets was considered in four references only (Li et al., 1996; Becker-Lemgau and Tacke, 1996; Zhang and Oeters, 1996; Davis et al., 1997), and Davis et al. (1997) alone explicitly modelled chemical reactions between gas and droplets. The presence of steam and hydrogen was considered in few models (Shinotake and Takamoto, 1993; Becker-Lemgau and Tacke, 1996; Davis et al., 1997). Finally, only in four cases was some form of validation explicitly mentioned (Gou et al., 1993; Shinotake and Takamoto, 1993; Schwarz and Davis, 1993; Davis et al., 1997).

MODEL DESCRIPTION

General Features

The model described here attempts to overcome the shortcomings of the previous models. It combines a CFD model of the phenomena in the gas phase (combustion, heat transfer from gas to the bath and refractories, and the heat, mass and momentum transfer between gas and droplets) and a heat and mass balance model for the bath. It is a finite-volume model, uses a colocated grid and is built using the CFX 4.2 package. The model is based on the following algorithm:

1. Perform heat and mass balances for the bath to initialise boundary conditions at the slag-gas boundary.
2. Iterate the gas-phase solution without the interaction between gas and droplets to establish consistent temperature and velocity fields.
3. Calculate the residence times and velocities of droplets in individual control volumes.
4. Perform heat and mass balances for the bath to update the boundary conditions at the slag surface.
5. Perform one iteration of the gas-phase solution including heat and mass transfer between gas and droplets.
6. Check if the solution has converged. If it has not, go to Step 3.

The model calculates:

- Coal, ore, flux and oxygen consumption;
- Post-combustion ratio;
- Heat-transfer efficiency;
- Off-gas temperature and composition;
- Heat transfer and chemical reactions between gas and iron and slag droplets; and
- Heat transfer between gas and bath, refractories and lance.

Assumptions

The following assumptions have been made:

- Process is steady state;
- Thermal conductivity and thickness of refractories are constant around the vessel;
- Temperature of slag surface is assumed 50 K higher than the bulk slag (Ibaraki et al., 1995);
- Temperature of gas generated in the bath is equal to the bulk slag and iron bath temperature;
- Post combustion takes place entirely in the freeboard;
- Pressure at the vessel mouth is atmospheric; and
- Because of the gas opacity, radiation heat loss through the vessel mouth is neglected (Healy and McBride, 1977).

Boundary Conditions

The following boundary conditions apply to the vessel walls and the outer surface of the lance: no-slip condition; no mass transfer between gas and walls; and wall functions are used to define the boundary conditions for flow and heat transfer at the walls (CFX 4.2, 1997). The mixed boundary condition is applied to the refractory walls to calculate the heat transfer from the hot face of refractories through the walls to the surroundings. There are two inlets: the lance tip, where the blast enters the freeboard through a single hole, and the slag surface, where gas from the bath enters the freeboard. The boundary conditions at the slag surface are as follows:

- Gas entering the freeboard consists of carbon monoxide, hydrogen and nitrogen generated in the bath and free moisture from raw materials which evaporates at the slag surface; and
- The flowrate and composition of gas entering the freeboard are calculated by the heat and mass balance model for the bath.

Conservation Equations

The formulation of the transport equations for the gas phase is taken from the CFX documentation (1997). The mass conservation and momentum transport equations are given by Eqs. (1) and (2), and the standard k-ε model of turbulence is used (Eqs. (3) and (4)).

$$\nabla \bullet \left(\rho \, \boldsymbol{u}\right) = S_m \tag{1}$$

$$\begin{aligned} &\nabla \bullet \left(\rho \;\; \boldsymbol{u} \times \boldsymbol{u} - \mu_{eff} \nabla \boldsymbol{u}\right) = \\ &-\nabla \left(p + \left(\frac{2}{3} \mu_{eff} - \zeta \right) \nabla \bullet \boldsymbol{u} \right) + \nabla \bullet \left(\mu_{eff} (\nabla \boldsymbol{u})^T \right) + S_u \end{aligned} \tag{2}$$

$$\nabla \bullet \left(\rho \, \boldsymbol{u} k - \mu_{eff} \nabla k\right) = G - \rho \varepsilon \tag{3}$$

$$\begin{aligned} &\nabla \bullet \left(\rho \, \boldsymbol{u} \varepsilon - \left(\mu_L + \frac{\mu_T}{1.217} \right) \nabla \varepsilon \right) = \\ &1.44 \frac{\varepsilon}{k} G - 1.92 \rho \frac{\varepsilon^2}{k} \end{aligned} \tag{4}$$

where the effective viscosity is calculated as:

$$\mu_{eff} = \mu_L + \mu_T \tag{5}$$

The mass fractions of species in the gas phase are calculated by transport equations of the form:

$$\nabla \bullet \left(\rho \, \boldsymbol{u} y_i - \rho \, D \nabla y_i \right) = S_{y_i} \tag{6}$$

The transport equation for enthalpy is given by:

$$\nabla \bullet \left(\rho \, \boldsymbol{u} H - \left(\frac{\lambda}{C_P} + \frac{\mu_T}{0.9} \right) \nabla H \right) = S_{rad} + S_D + S_d \tag{7}$$

The radiation model is based on the P_1 spherical harmonics approximation (Ozisik, 1975). Droplet dynamics, heat transfer and the rate of chemical reactions between gas and droplets are calculated as in Panjkovic et al. (1996, 1999). The droplet source terms in the transport equations are included using the particle-source-in-cell technique (Crowe et al., 1977). The dust is assumed to be heated from the bath temperature to the gas temperature at the vessel mouth. The enthalpy difference is then split between the control volumes in proportion to their volume.

The eddy-break-up model was employed for the combustion modelling. Also, equilibrium for the water-gas-shift reaction is assumed in this model. This assumption was used in calculating the mass fractions of CO, CO_2, H_2, H_2O, N_2 and O_2 by applying a modified approach of Haywood et al. (1994), with transport equations solved for atomic carbon, oxygen and hydrogen and for molecular oxygen and nitrogen.

Model Parameters

The vessel dimensions are shown in Fig. 2 and approximate the Nippon Steel 100 t pilot plant (NSC100) (Ibaraki et al., 1995). Most simulation parameters are given in Panjkovic et al. (1996). The standard conditions specific to the CFD model are: temperature of the lance surface is 600 ^oC; lance tip 1.8 m above the bath, its inner diameter 0.15 m; the blast velocity 318.4 m s^{-1}; and the apparent density of the foaming slag 800 kg m^{-3}. In the absence of reliable formulae for the size of the cavity formed in slag by the oxygen jet, the cavity was taken to be the "average" of those presented by Shinotake and Takamoto (1992) and Katayama et al. (1992). It is an inverted frustum, with top and bottom surfaces of radii 1.4 m and 0.3 m, respectively, and a depth of 1.6 m.

The main criterion in selecting the grid was that a further refinement did not change results significantly. In most of the domain the turbulent dimensionless distance y_w^+ was between 30 and 300. The grid contains 3098 control volumes and the calculation domain is half of the axisymmetric axial-radial plane (Panjkovic, 1999).

RESULTS

Validation Tests

Validation tests were performed with three sets of data from the NSC100. The production rate in the model was matched to the particular trial and the flowrate of oxygen for post combustion was adjusted so that the calculated PCR matched the measured one. It must be conceded that these tests are incomplete for this complex model. Unfortunately, measurements of velocity, temperature and composition profiles in the freeboard of an iron-bath reactor are not available. Results are summarised in Table 1. It can be seen that the match with measured data is reasonable. However, the difference between measured and calculated HTE is pronounced. It is difficult to explain the difference without detailed information on the temperature measurements at the NSC100 and the formula for HTE that was used in NSC. Some additional means to enhance heat transfer from gas to the bath and droplets should be considered, such as smaller diameter slag droplets than assumed in the simulations, and greater effective surface area for heat transfer to the bath. Either the bath surface area is larger than assumed, due to foaming and surface waves, or a fraction of post combustion occurs in the foaming slag.

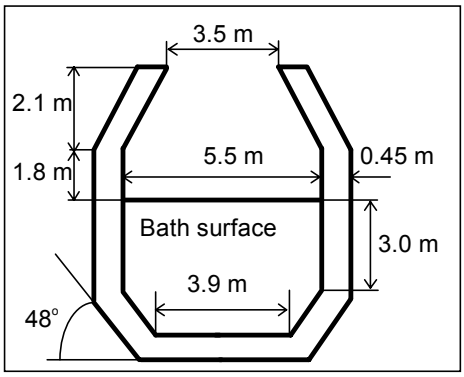

Figure 2. Vessel dimensions (Ibaraki et al., 1995).

The Impact of Lance Height

Only this sensitivity test is presented here (other sensitivity tests are given in Panjkovic, 1999). Since the lance height influences the cavity size, the formulae given by Cheslak et al. (1969) were used to estimate the changes in the cavity size relative to the standard case. The lance heights considered were the standard case and ±20 % variations on the standard case. The results obtained for different cases are compared in Table 2. The gas temperature falls near the cavity wall with higher lance position, but rises above bath surface outside the cavity, referred to as the flat bath (Fig. 3). This causes the radiation transfer rate to the flat bath to rise, which partially offsets the fall in the radiation heat transfer to the cavity. Convection heat transfer to the bath shows little change with increasing lance height, but heat transfer from gas to droplets increases sharply due to the rise in gas temperature above the flat bath where the majority of droplets are located. The increase in heat transfer to droplets improves HTE and causes coal consumption to decrease. The rise in gas temperature above the flat bath and the higher partial pressure of oxidising gases, cause the rate of chemical reactions between gas and droplets to increase. Lower coal consumption means that less gas is generated in the bath which, at constant flowrate of oxygen for post combustion, results in higher PCR. Despite the increase in PCR, the off-gas temperature decreases due to the improved heat transfer from gas to droplets.

Comparison to a Simpler Model

It is interesting to compare the results of the CFD model to those obtained with a simpler heat and mass balance (HMB) model (Panjkovic et al., 1996). The principal difference between the models is that the HMB model assumes spatial uniformity of gas velocity, temperature and composition, and uses a single-gas-zone model for calculating heat transfer in the freeboard. The results of the validation tests with the two models are similar (Table 3). The comparison was conducted using the same data. The heat losses to the lance calculated by the CFD model were specified in the HMB model, and the bath surface area in the HMB model was the same as in the CFD model. The comparison between two models shows the following:

1. The main difference is the much higher rate of chemical reactions between gas and droplets calculated by the HMB model. The uniformity of gas properties means that all droplets are exposed to gas at the temperature and composition of the off-gas. In the CFD model the gas temperature (Fig. 3) and partial pressure of oxidising gases are relatively low over the flat bath, where most droplets are located. This also explains the lower heat transfer from gas to droplets calculated by the CFD model.
2. The coal consumption calculated by two models is similar. The total heat transfer from gas to the bath and droplets is slightly higher with the HMB model. However, this is offset by the higher rate of oxidation and decarburisation of iron droplets.
3. The HTE calculated by the CFD model is consistently lower than for the HMB model. The reason is the estimation of the heat released by post combustion, required to calculate HTE. The amount of CO_2 and H_2O created by post combustion is calculated from the flowrate of these species in the off-gas and the rate at which they are consumed by decarburisation and reoxidation reactions. The rate of these reactions is calculated higher by the HMB model.
4. The models calculate similar values of heat losses to the refractory walls surrounding the freeboard. Also, the difference between the calculated radiation heat transfer to the bath is reasonably small (4-14 %). This suggests that the single-gas-zone radiation model used in the HMB model is a reasonable approximation.
5. The most important mechanisms for heat transfer from gas to bath are radiation to the bath and convection to droplets. Convection heat transfer to the bath is only about 10 % of the total heat transfer to the bath and droplets, as calculated by the CFD model. Radiation heat transfer to droplets accounts for about 20 % of the total heat transfer to droplets.

CONCLUSION

The performance of an iron-bath reactor have been studied using a comprehensive numerical model which combines a computational fluid dynamics approach for the gas phase and a heat and mass balance model for the bath. The model was validated with data reported by the Nippon Steel Corporation for a 100 t pilot plant. The calculated coal consumption and off-gas temperature tend to be higher than measured, and the HTE is significantly lower than measured. The most likely causes of the discrepancies between the measured and the calculated values are the uncertainties in the size and generation rate of droplets, little understanding of the combustion and heat transfer in the foaming slag, and the assumed shape of the bath surface. Radiation to the slag surface and convection heat transfer to droplets are the dominant mechanisms of heat transfer from gas to the bath. Chemical reactions between gas and iron droplets (decarburisation and reoxidation) have a strong influence on the post-combustion ratio, while reoxidation of slag is less important. The lance height was found to have a significant impact on coal consumption.

ACKNOWLEDGEMENTS

This work was carried out with the support of BHP Steel and the ARC whilst one of the authors (VP) was a graduate student at the University of New South Wales, Sydney. The authors wish to thank BHP Steel for permission to publish this paper.

	NSC100	model	NSC100	model	NSC100	model
Coal consumption [kg tHM^{-1}] 1)	1180	1181	1060	1114	1120	1240
HTE [%]	89	81	96	80	90	74
Total O_2 consumption [m^3 at STP tHM^{-1}] 2)	885	885	874	857	824	950
Off-gas temperature [K]	1900-2200	2206	1900-2200	2275	1900-2200	2358
Production [tHM h^{-1}]	22.6		24.5		36.4	
PCR [%]	42		46		42	

1) tHM: ton of hot metal

2) STP: standard temperature and pressure (273.15 K and 101.3 kPa, respectively)

Table 1. Comparison between CFD model calculations and data from experiments at the NSC100 (Ibaraki et al., 1995). PCR and HTE are defined as in Panjkovic et al. (1996).

Lance position	lower (1.44 m)	standard case	higher (2.16 m)
Coal consumption [kg tHM^{-1}]	1366	1248	992
PCR [%]	38.7	41.7	52.1
HTE [%]	71.5	74.4	79.2
Off-gas temperature [K]	2369	2353	2343
Decarburisation rate of iron [mole s^{-1}]	10.0	13.8	19.3
Reoxidation rate of iron [mole s^{-1}]	3.6	8.2	10.2
Reoxidation rate of Fe^{2+} [mole s^{-1}]	0.6	1.2	2.6
Heat losses to the walls and lance [MW]	3.8	3.2	2.7
Convection heat transfer to the bath [MW]	7.2	7.6	7.3
Radiation heat transfer to the bath [MW]	34.8	34.7	33.4
Heat transfer from gas to droplets [MW]	25.9	28.1	34.9

Table 2. Results obtained with three different values of lance height.

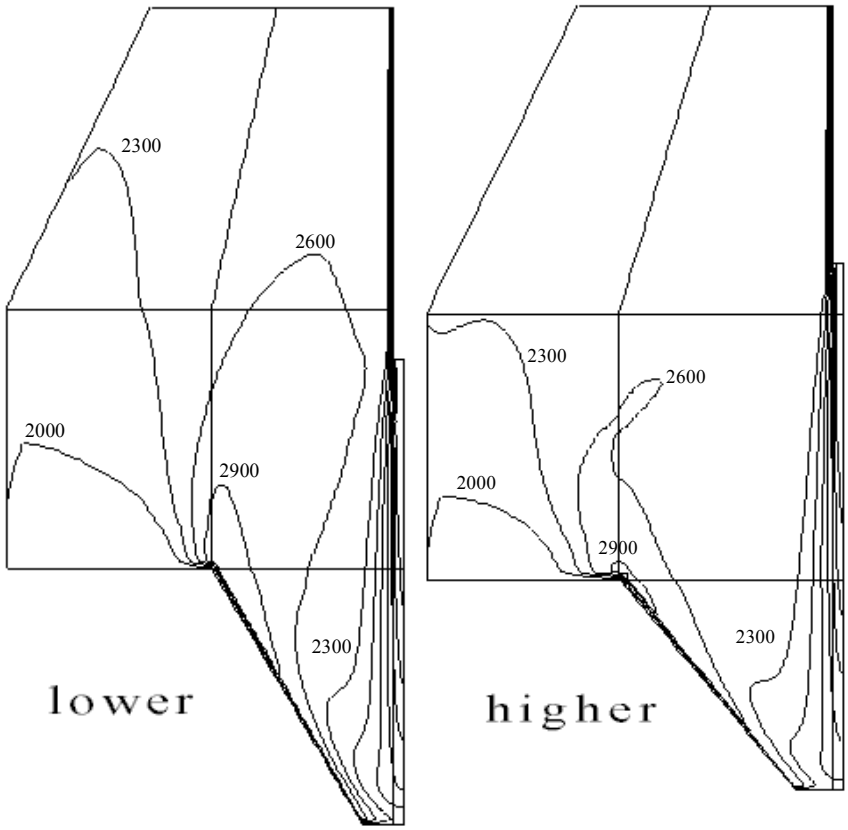

Figure 3. Temperature contours (K) for different values of lance height.

	Case 1		Case 2		Case 3	
	HMB	CFD	HMB	CFD	HMB	CFD
Coal consumption [kg tHM^{-1}]	1205	1181	1115	1114	1237	1240
PCR [%]	42	42	46	46	42	42
HTE [%]	82	81	82	80	77	74
Oxy. consumption [m^3 at STP tHM^{-1}]	911	885	860	857	945	950
Off-gas temperature [K]	2241	2206	2274	2275	2337	2358
Decarburisation rate [mol s^{-1}]	16.6	9.9	17.7	11.9	23.1	13.9
Reoxidation rate of iron [mol s^{-1}]	40.5	5.6	42.7	8.7	37.0	8.5
Reoxidation rate of Fe^{2+} [mol s^{-1}]	2.9	1.0	3.2	1.2	3.3	1.2
Heat losses to the refractory walls and lance [MW]	3.6	3.5	3.8	3.7	4.3	4.1
Convection heat transfer to the bath [MW]	-	4.3	-	4.4	-	7.5
Radiation heat transfer to the bath [MW]	23.3	25.0	25.6	26.7	30.3	34.7
Heat transfer from gas to droplets [MW]	22.3	16.1	24.5	18.8	40.8	28.3

Table 3. A comparison of results obtained with the CFD and HMB models.

REFERENCES

AI, J., WANG, D. and XIE, Y. (1990), "System Simulation of the Smelting Reduction Process", *Proc. Smelt. Reduction & Near-net Shape Casting,* Korean Institute of Metals, Pohang, South Korea, **1**, 130-39.

BECKER-LEMGAU, U. and TACKE, K.-H. (1996), "Mathematical Model for Post Combustion in Smelting Reduction", *Steel Res*., **67**, 127-37.

CFX 4.2 Flow Solver User Guide (1997), AEA Technology, Harwell, UK.

CHESLAK, F.R, NICHOLLS, J.A. and SICHEL, M. (1969), "Cavities Formed on Liquid Surfaces by Impinging Gaseous Jets", *J. Fluid Mech*., **36**, 55-63.

CROWE, C.T., SHARMA M.P. and STOCK, D.E. (1977), "The Particle-source-in-cell (PSIC) Model for Gas-droplet Flows", *ASME J. Fluids Eng*., **99**, 325-32.

DAVIS, M.P., PERICLEOUS, K., SCHWARZ M.P. and CROSS, M. (1997), "Mathematical Modelling Tools for the Optimisation of Direct Smelting Processes", *Proc. Int. Conf. on CFD in Minerals and Metal Processing and Power Generation,* CSIRO, Melbourne, 25-39.

FRUEHAN, R.J., ITO, K. and OZTURK, B. (1989), "Analysis of Bath Smelting Processes for Producing Iron", *Steel Res*., **60**, 129-37.

GOU, H.Y., IRONS, G.A. and LU, W.-K. (1993), "Mathematical Modelling of Post Combustion in a KOBM Converter", *Metall. Trans. B*, **24B**, 179-88.

HAYWOOD, R.J., TRUELOVE, J.S. and McCARTHY, M.J. (1994), "Modelling of Pulverised Coal Injection and Combustion in Blast Furnaces", *Proc. 53rd ISS-AIME Ironmaking Conf.,* Chicago, 437-42.

HEALY, G.W. and McBRIDE, D.L. (1977), "The Mass-energy Balance", BOF Steelmaking Vol. 4: Operation, AIME, PA, 101-70.

IBARAKI, T., YAMAUCHI, M., SAKAMOTO, Y., HIRATA, H. and KANEMOTO, M. (1995), "Experimental Operation of Smelting Reduction with a 100 mt Smelter - I. Operation and the Slag in the Smelter", *I&SM*, **22**, 3, 83-90.

KATAYAMA, H., OHNO, T., YAMAUCHI, M., MATSUO, M., KAWAMURA, T. and IBARAKI, T. (1992), "Mechanism of Iron Oxide Reduction and Heat Transfer in the Smelting Reduction Process with a Thick Layer of Slag", *ISIJ Int*., **32**, 95-101.

LI, B., HE, Y. and SAHAI, Y. (1996): "Study on the Post Combustion in BOF", *Proc. Int. Conf. on Modelling and Simulation in Metal. Eng. and Mat. Sci.,* Chinese Society of Metals, Beijing, 297-303.

OZISIK, M.N. (1973), "Radiative Transfer and Interactions with Conduction and Convection", John Wiley and Sons, New York.

PANJKOVIC, V., OSTROVSKI, O., TRUELOVE, J. and CRIPPS CLARK, C. (1996), "Mathematical Modelling of the Smelting Reduction of Iron: The Effect of Properties of Raw Materials and Blast Injection", *Proc. Howard Warner Int. Symp. on Injection in Pyrometallurgy,* G.K. Williams CRC, Melbourne, 399-413.

PANJKOVIC, V. (1999), "Numerical Modelling of Gas Phase Phenomena and Fuel Efficiency in Iron-bath Reactors", PhD Thesis, The University of NSW, Sydney, Australia.

PANJKOVIC, V., TRUELOVE, J. and OSTROVSKI, O. (1999): "Numerical Modelling of Gas Phase Phenomena and Fuel Efficiency in Iron-bath Reactors", *58th ISS-AIME Ironmaking Conf.*, Chicago, 431-42.

SAMPAIO, R.S., FRUEHAN, R.J. AND OZTURK, B. (1992), "Rate of Coal Devolatilization in Iron and Steelmaking Processes, Part II.", *I&SM*, **19**, 8, 59-66.

SCHWARZ, M.P. and DAVIS, M.P. (1993), "Simulation of the CMU Iron Bath Reactor", *REP824*. CSIRO, Institute of Minerals, Energy and Construction, Division of Mineral and Process Engineering.

SHIN, M.K., LEE, S.D., JOO, S.H. and YOON, J.K. (1993), "A Numerical Study of the Combustion Phenomena Occurring at the Post Combustion Stage in Bath-type Smelting Reduction Furnace", *ISIJ Int*., **33**, 369-75.

SHINOTAKE, A. and TAKAMOTO, Y. (1992), "Numerical Analysis of Combustion Mechanism in Iron Bath Smelting Reduction Furnace", *Tetsu-to-Hagane*, **78**, 1250-57.

SHINOTAKE, A. and TAKAMOTO, Y. (1993), "Combustion and Heat Transfer Mechanism in Iron Bath Smelting Reduction Furnace", *Rev. Metall. - CIT*, **90**, 965-73.

TANSKI, J.A. (1994), "Numerical Simulation of the AISI Bath Smelter", Center for Iron and Steel Research Progress Report. Carnegie Mellon University. October, 35-51.

XU, S. and HOLAPPA, L. (1990), "Modelling of Energy Relations in Smelting Reduction", *Proc. Smelt. Reduction & Near-net Shape Casting,* Korean Institute of Metals, Pohang, South Korea, **1**, 237-46.

ZHANG, L. and OETERS, F. (1991), "A Model of Post Combustion in Iron-bath Reactors, Part 1: Theoretical Basis", *Steel Res*., **62**, 95-106.

ZHANG, L. and OETERS, F. (1993), "A Model of Post Combustion in Iron-bath Reactors, Part 3: Theoretical Basis for Post Combustion with Preheated Air", *Steel Res*., **64**, 542-48.

ZHANG, L. and OETERS, F. (1996), "Modelling of Post-combustion in a Foamy Slag by Smelting Reduction", *Proc. Int. Conf. on Modelling and Simulation in Metal. Eng. and Mat. Sci.,* Chinese Society of Metals, Beijing, 390-96.